

High-pressure behaviour of studtite, $\text{UO}_4 \cdot 4\text{H}_2\text{O}$, and metastudtite, $\text{UO}_4 \cdot 2\text{H}_2\text{O}$ - a Raman investigation

S. Labs¹, J.D. Bauer², B. Winkler², L. Bayarjargal², H. Curtius¹, D. Bosbach¹.

¹Forschungszentrum Jülich GmbH, Institute of Energy and Climate Research - IEK-6, D-52428 Jülich.

²Goethe-Universität Frankfurt am Main, Institut für Geowissenschaften, Abt. Kristallographie, Altenhöferallee 1, D-60438 Frankfurt am Main.

Introduction

Studtite, $\text{UO}_4 \cdot 4\text{H}_2\text{O}$, and metastudtite, $\text{UO}_4 \cdot 2\text{H}_2\text{O}$, are the only peroxide containing minerals occurring in nature^[1]. They appear associated with uraninite (UO_2), which can be regarded as natural analogon to spent nuclear fuel (SNF). Kubatko et al. discussed, that there are certain conditions under which the local environment becomes oxidizing even if overall conditions are reducing^[2]. Therefore, especially studtite, could play an important role as an alteration phase of SNF in a deep geological repository. Studtite as well as metastudtite could be found as secondary phases of SNF in a two year experiment with water^[3]. Formation of metastudtite on UO_2 samples was observed by Sattomay et al. as direct effect of alpha-radiolysis of water^[4]. After the first 10000 years, mainly α -radiation will be present in a nuclear repository. While most studies on the safety assessment emphasize on the silicates, it has been demonstrated by Forbes et al.^[5] that some of these earlier formed phases are susceptible to alteration to studtite.



Fig. 1: studtite, metastudtite and amorphous UO_3 (dehydration product)

While the structure of studtite has been determined from single crystal data^[6], that of metastudtite still remains speculative. Very little data on the reaction of studtite to metastudtite and further to amorphous UO_3 is available. The involved mechanisms are scarcely investigated.

Experimental

Studtite was synthesized from an acidic aqueous UO_2 suspension by slowly adding 30 % H_2O_2 solution. After reaction the light yellow precipitate was filtered and then dried at ambient temperature.

Metastudtite was obtained by dehydrating the prepared studtite at 90 °C for 48 hrs. Phase purity was checked by powder XRD.

High-pressure studies were performed with a Boehler-Almax type diamond-anvil-cell (DAC)^[9], employing a pre-indented tungsten gasket with 140 μm laser drilled hole and using Ne as quasi-hydrostatic pressure medium. Pressures were determined during the experiment by the ruby fluorescence method^[10].

Analytical Equipment

X-ray diffraction D8 by Bruker AXS GmbH using Cu K α , VarnTec detector, ($\Delta 2\theta = 0.021$, $2\theta = 10 - 130^\circ$, $t = 5$ s/step).

Confocal micro-Raman Spectroscopy Renishaw Raman System (RM-1000) using a Nd:YAG laser, $\lambda = 532$ nm.

Transmission Electronmicroscopy Philips CM300 FEG/UT – STEM with 300 kV acceleration voltage.

Results

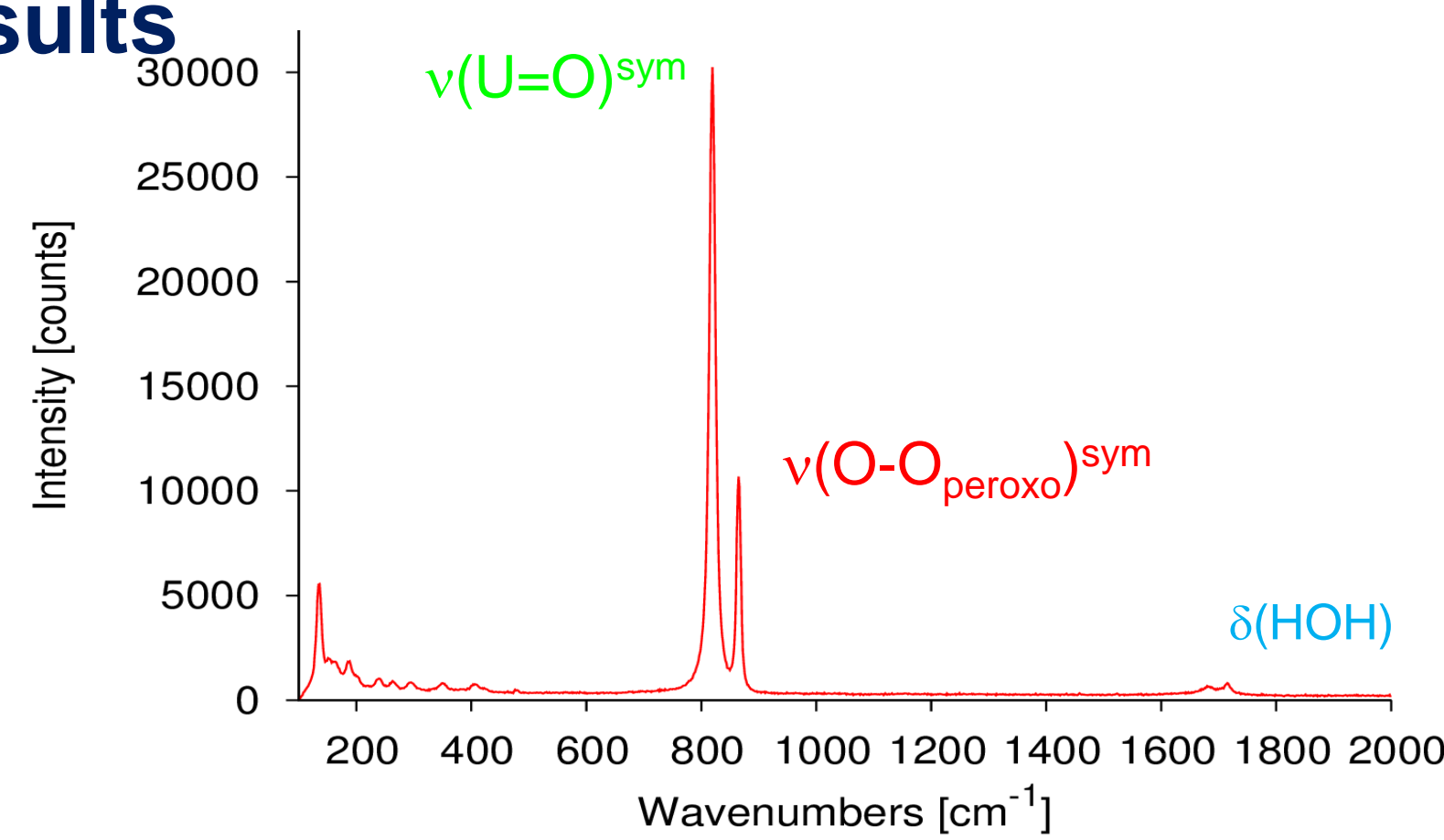


Fig. 2: Raman spectrum of studtite at ambient pressure, symmetric $\nu(\text{U=O})^{\text{sym}}$ and $\nu(\text{O-O-peroxo})^{\text{sym}}$ vibration are visible as strongest peaks (assignments according to [7]).

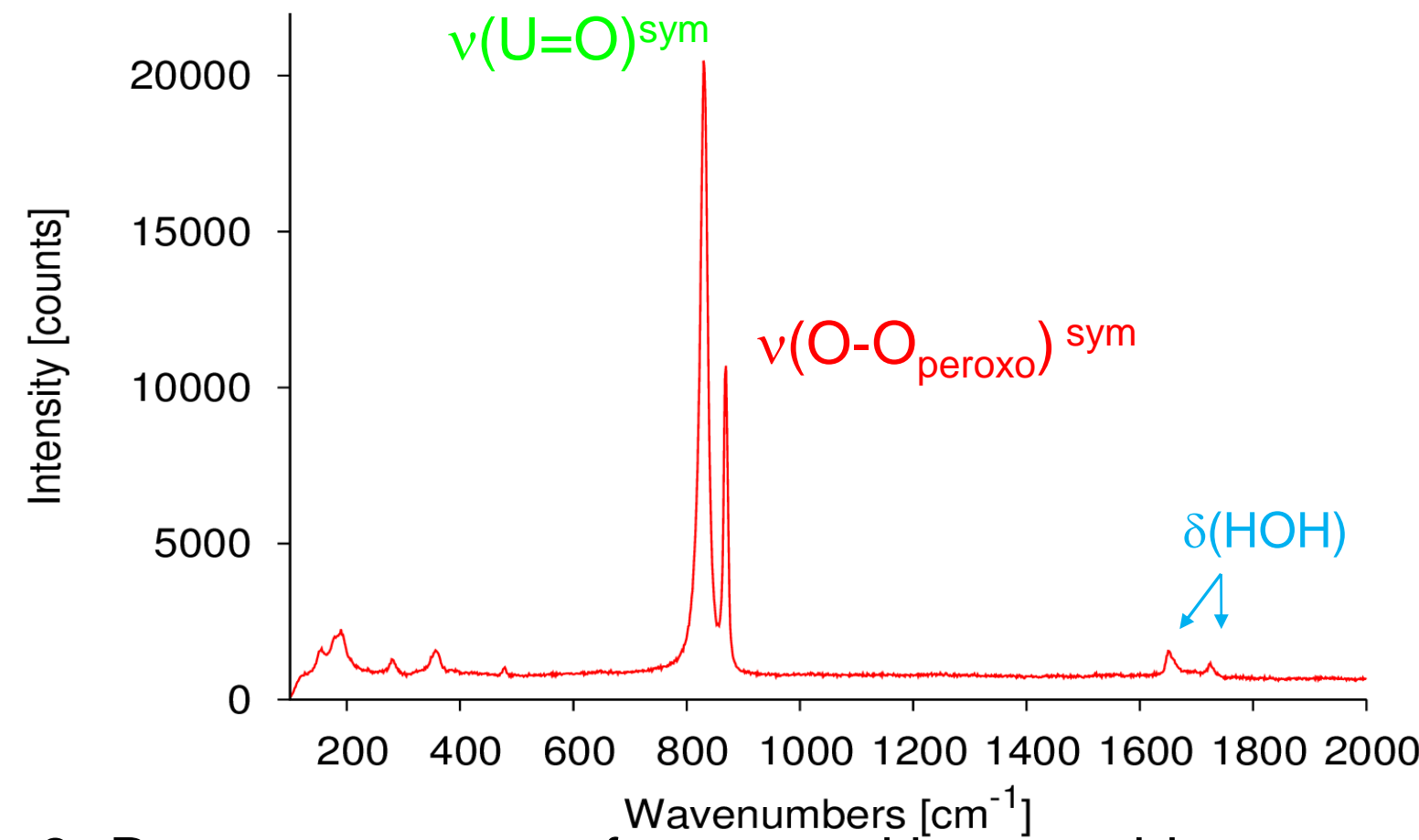


Fig. 3: Raman spectrum of metastudtite at ambient pressure $\delta(\text{HOH})$ bending vibration is more distinguished than in studtite (cf. fig. 2).

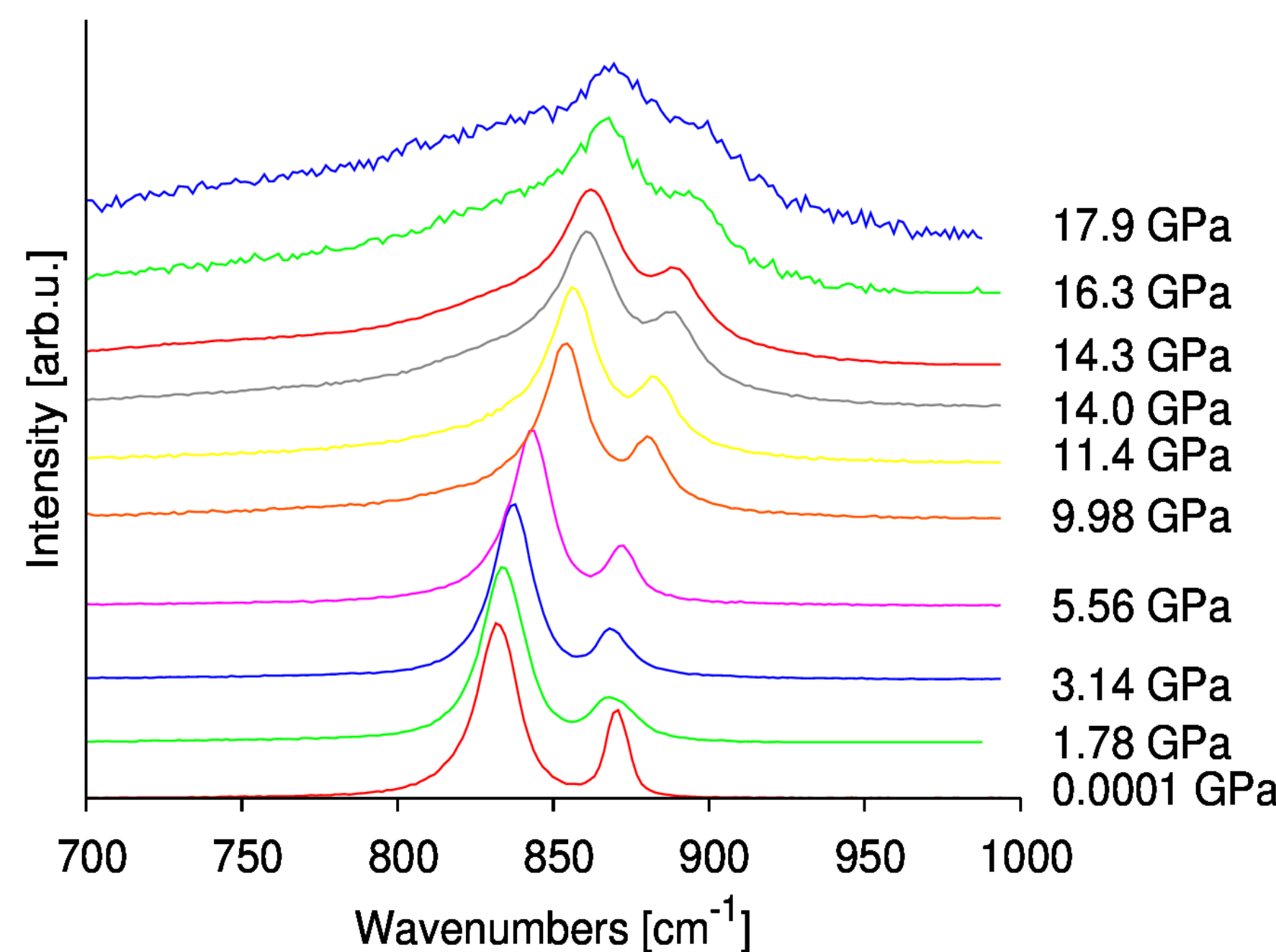
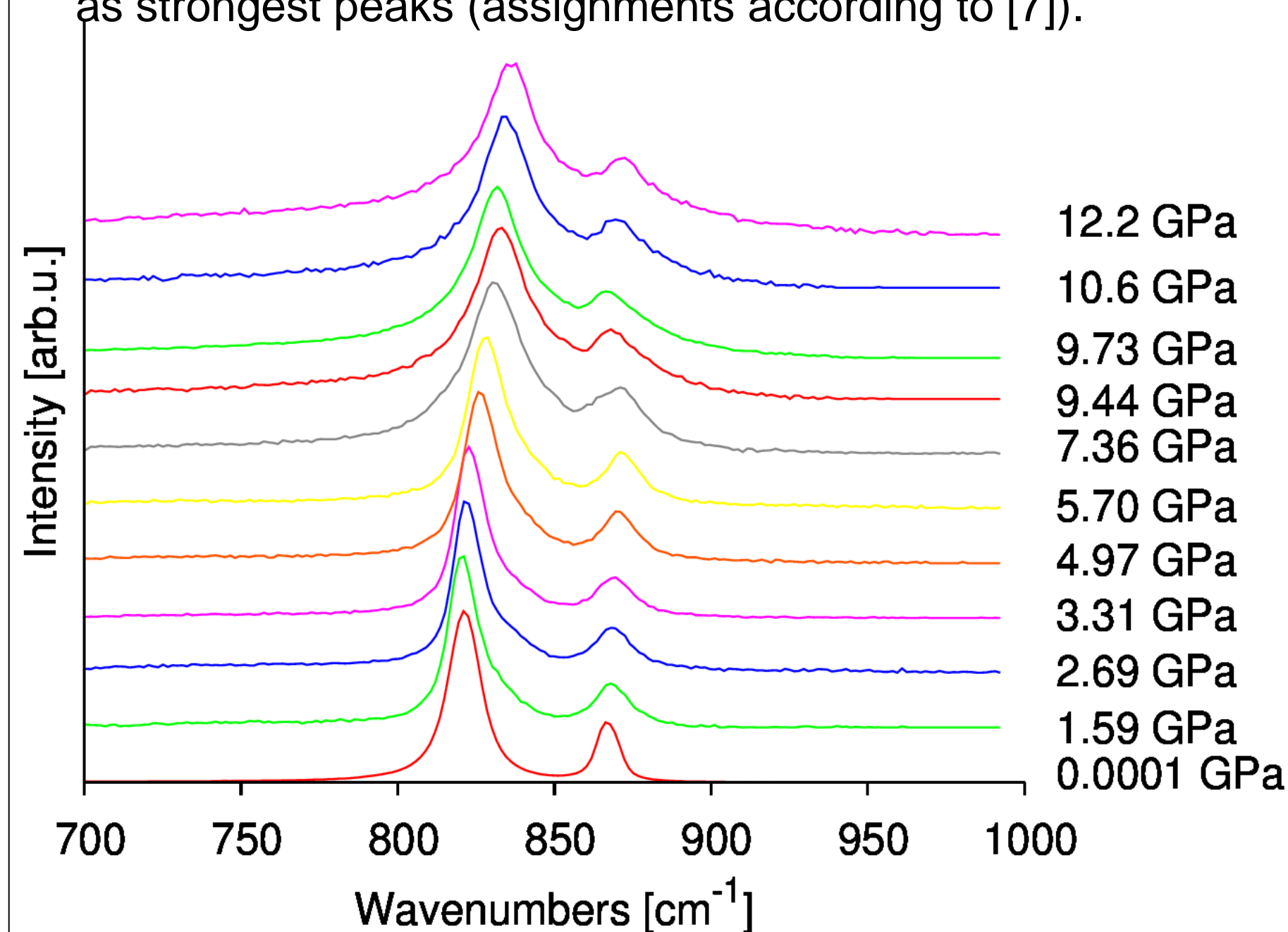


Fig. 4: Close up of the region 700 – 1000 cm^{-1} showing the symmetrical stretching vibration $\nu(\text{U=O})^{\text{sym}}$ and $\nu(\text{O-O-peroxo})^{\text{sym}}$ in studtite (left) and metastudtite (right) shift towards higher wavenumbers with increasing pressure. Above 16 GPa the signals in metastudtite become significantly broader, suggesting amorphization.

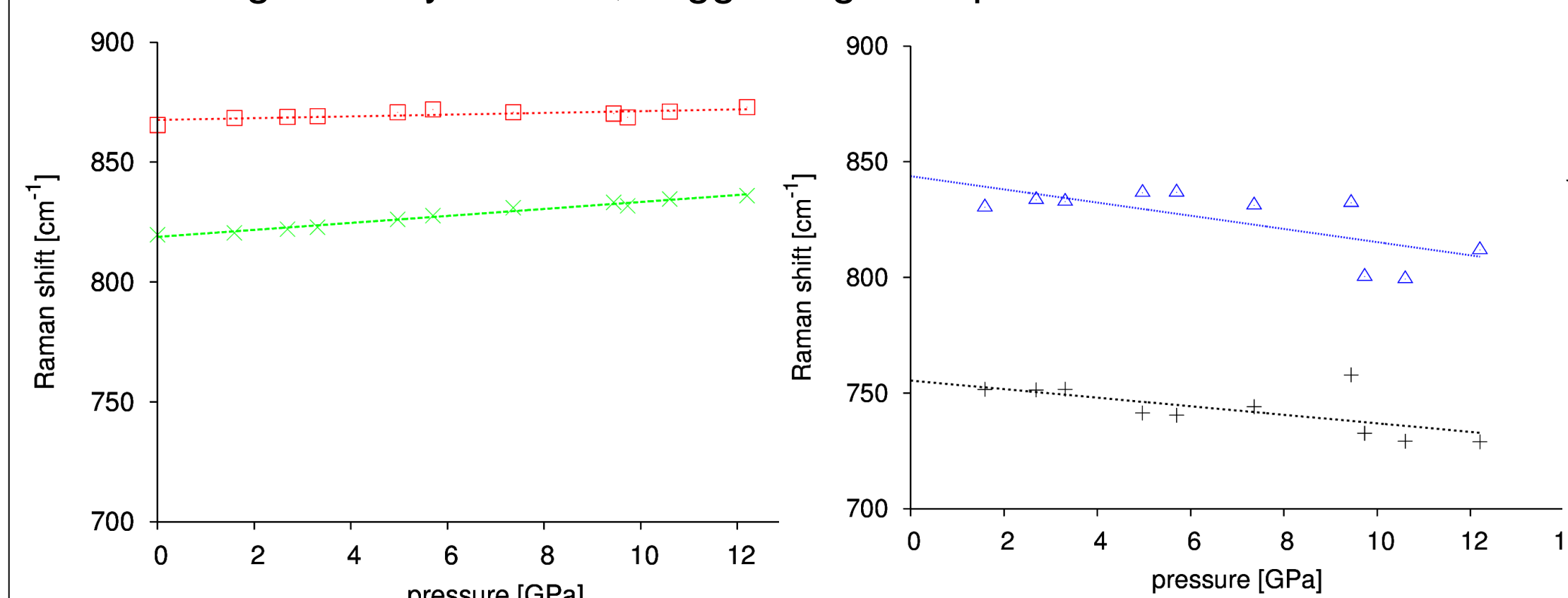


Fig. 6: Raman shifts and linear fit of $\nu(\text{U=O})^{\text{sym}}$ and $\nu(\text{O-O-peroxo})^{\text{sym}}$ in studtite with increasing pressure. Weak stretching vibration $\nu(\text{U-O})$ and $\nu(\text{U-O-U-O})$ long range vibrations [8] already appear at rather low pressures, above 1.6 GPa. Especially the $\nu(\text{U-O-U-O})$ long range vibration can be associated with beginning decomposition to UO_3 .

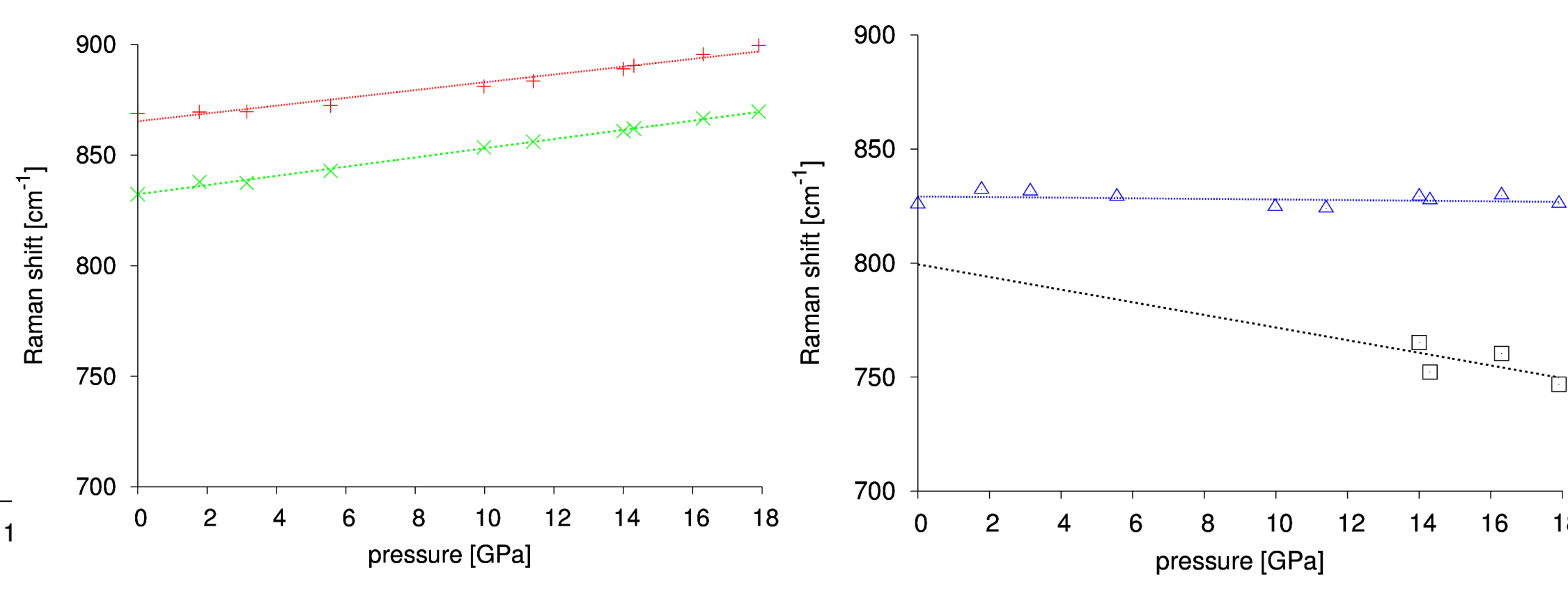


Fig. 7: Raman shifts and linear fit of $\nu(\text{U=O})^{\text{sym}}$ and $\nu(\text{O-O-peroxo})^{\text{sym}}$ in metastudtite with increasing pressure are larger than in studtite. $\nu(\text{U-O})$ stretching vibration is present from beginning, while the $\nu(\text{U-O-U-O})$ long range is visible only above 14 GPa (cf. fig. 4)

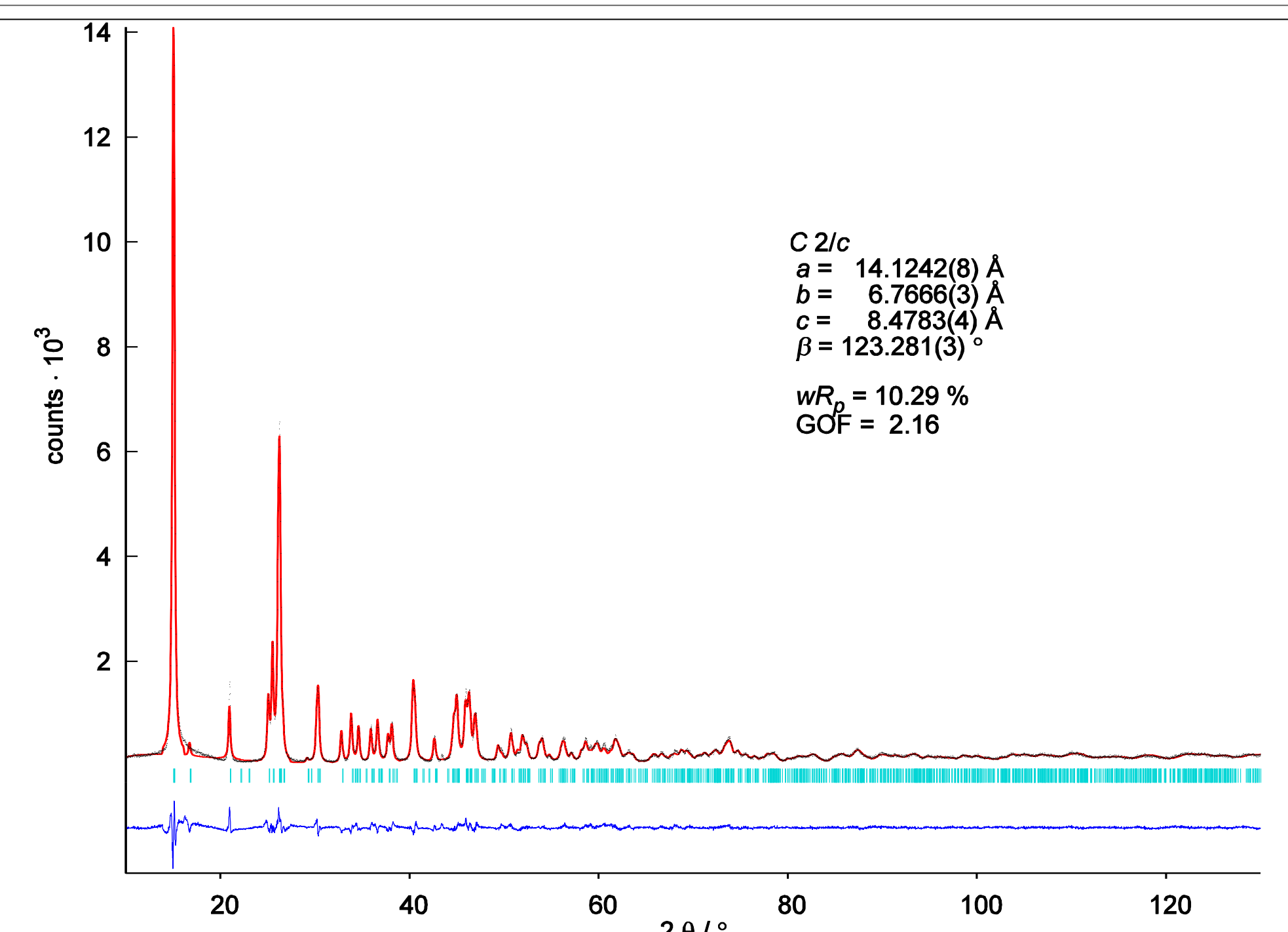


Fig. 8: Rietveld refinement of studtite powder XRD data shows one pure phase.

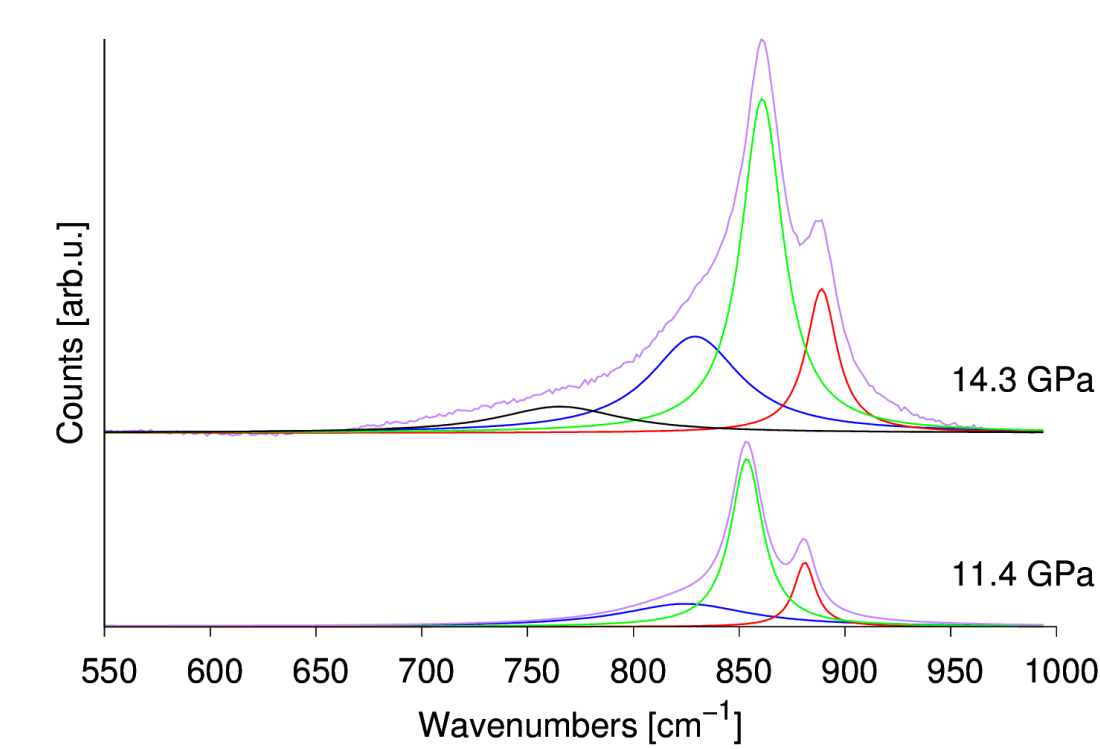


Fig. 5: Example fits of $\nu(\text{U=O})^{\text{sym}}$, $\nu(\text{O-O-peroxo})^{\text{sym}}$, $\nu(\text{U-O})$ stretching and $\nu(\text{U-O-U-O})$ long range vibrations in metastudtite.

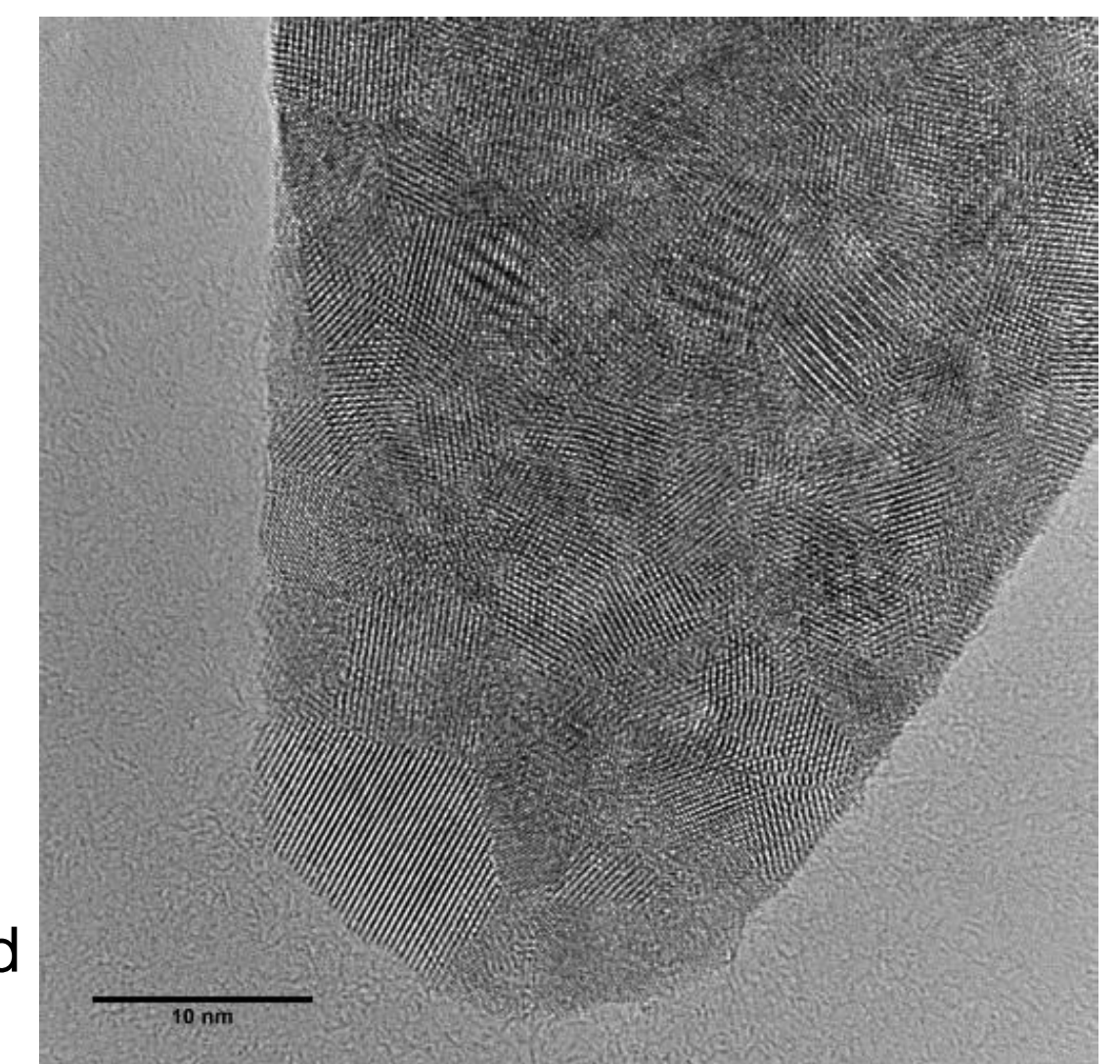


Fig. 9: HRTEM image of metastudtite. The particle exhibits several small grains with a grainsize around 10 nm.

	ν_0 [cm^{-1}]	$d\nu/dp$ [$\text{cm}^{-1}/\text{GPa}$]	assignment
Studtite	819	1.46 ± 0.07	$\nu(\text{U=O})^{\text{sym}}$
	866	0.37 ± 0.12	$\nu(\text{O-O-peroxo})^{\text{sym}}$
Meta-studtite	833	2.08 ± 0.05	$\nu(\text{U=O})^{\text{sym}}$
	866	1.76 ± 0.12	$\nu(\text{O-O-peroxo})^{\text{sym}}$

Tab. 1: Position and pressure shifts (derived from linear fit, cf. figs. 6 and 7) of the two strongest vibrations in studtite and metastudtite.

Conclusion

- High pressure Raman data of studtite and metastudtite have been collected for the first time
- Position and pressure shifts were determined for the two strongest peaks in studtite and metastudtite which can be assigned to the $\nu(\text{U=O})^{\text{sym}}$ and $\nu(\text{O-O-peroxo})^{\text{sym}}$ stretching vibrations.
- The $\nu(\text{U=O})^{\text{sym}}$ vibration is at ambient conditions 14 cm^{-1} higher in metastudtite than in studtite, corresponding to a stronger U=O – bond in metastudtite.
- In both samples $\nu(\text{U=O})^{\text{sym}}$ and $\nu(\text{O-O-peroxo})^{\text{sym}}$ shift to higher wavenumbers during compression, suggesting a strengthening in U-O – bonding.
- Metastudtite shows decomposition to UO_3 at higher pressures than studtite and hence higher pressure stability.

- HRTEM images reveal a very small crystallite size in both compounds. Whereas metastudtite remains stable in the electron beam at 300 kV, studtite rapidly undergoes dehydration. Size and position of crystallite grains remains the same.

- There is no evidence so far for a pressure induced phase transition of studtite to metastudtite.

References

- [1] K. Walenta, On studtite and its composition, *Amer. Min.* **59** (1974) 166 – 171. [2] K.-A. Kubatko et al. Stability of Peroxide-Containing Uranyl Minerals, *Science* **302** (2003) 1191-1193. [3] B. Hanson et al. Corrosion of commercial spent nuclear fuel. 1. Formation of studtite and metastudtite, *Radiochim. Acta*, **93** (2005) 159-168. [4] G. Sattomay et al. Alpha-radiolysis effects on UO_2 alteration in water, *J. Nuc. Mat.* **288** (2001) 11-19. [5] T. Forbes et al. Alteration of dehydrated schoepite and soddyite to studtite, $[(\text{UO}_2)(\text{O}_2)(\text{H}_2\text{O})_2]$, *Amer. Min.* **96** (2009) 449-458. [6] P.C. Burns et al. Studtite: $[(\text{UO}_2)(\text{O}_2)(\text{H}_2\text{O})_2]$. The first structure of a peroxide mineral, *Amer. Min.*, **88** (2003) 1165-1168. [7] S. Bastians, Raspite and studtite: Raman spectra of two unique minerals, *J. Raman Spectrosc.*, **35** (2004) 726-731. [8] M. Lipp et al., Raman investigation of the uranium compounds U_3O_8 , UF_4 , UH_3 and UO_3 under pressure at room temperature, LLNL-TR-522251 (2011). [9] R. Boehler, New diamond cell for single-crystal x-ray diffraction, *Rev. Sci. Instrum.* **77** (2006) 115103. [10] H.K. Mao and P.M. Bell, Calibration of the ruby pressure gauge to 800 kbar under quasi-hydrostatic conditions, *J. Geophys. Res.* **91** (1986) 4673.

Acknowledgment

We gratefully acknowledge that financial support from German Federal Ministry of Education and Research (BMBF), ImmoRad Project (Grant No. 02NUK019E) has been received.